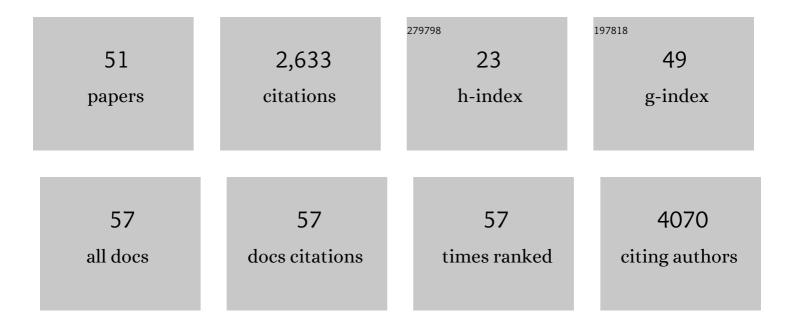
Shukuan Ling

List of Publications by Year in descending order

Source: https://exaly.com/author-pdf/4608566/publications.pdf Version: 2024-02-01



SHURLANLING

#	Article	IF	CITATIONS
1	The mechanosensitive IncRNA Neat1 promotes osteoblast function through paraspeckle-dependent Smurf1 mRNA retention. Bone Research, 2022, 10, 18.	11.4	22
2	Anoctamin 1 controls bone resorption by coupling Clâ^' channel activation with RANKL-RANK signaling transduction. Nature Communications, 2022, 13, .	12.8	15
3	The coupling of reduced type H vessels with unloading-induced bone loss and the protection role of Panax quinquefolium saponin in the male mice. Bone, 2021, 143, 115712.	2.9	12
4	Breast cancer exosomes contribute to pre-metastatic niche formation and promote bone metastasis of tumor cells. Theranostics, 2021, 11, 1429-1445.	10.0	163
5	Casein Kinase-2 Interacting Protein-1 Regulates Physiological Cardiac Hypertrophy via Inhibition of Histone Deacetylase 4 Phosphorylation. Frontiers in Physiology, 2021, 12, 678863.	2.8	2
6	3′ untranslated region of <i>Ckip-1</i> inhibits cardiac hypertrophy independently of its cognate protein. European Heart Journal, 2021, 42, 3786-3799.	2.2	9
7	Targeting E3 Ubiquitin Ligase WWP1 Prevents Cardiac Hypertrophy Through Destabilizing DVL2 via Inhibition of K27-Linked Ubiquitination. Circulation, 2021, 144, 694-711.	1.6	31
8	WWP1 Deficiency Alleviates Cardiac Remodeling Induced by Simulated Microgravity. Frontiers in Cell and Developmental Biology, 2021, 9, 739944.	3.7	9
9	Vascular smooth muscle cellâ€specific miRNAâ€⊋14 knockout inhibits angiotensin IIâ€induced hypertension through upregulation of Smad7. FASEB Journal, 2021, 35, e21947.	0.5	7
10	Ckip-1 3′-UTR Attenuates Simulated Microgravity-Induced Cardiac Atrophy. Frontiers in Cell and Developmental Biology, 2021, 9, 796902.	3.7	2
11	Knockdown of CD44 inhibits the alteration of osteoclast function induced by simulated microgravity. Acta Astronautica, 2020, 166, 607-612.	3.2	8
12	miR-214 stimulated by IL-17A regulates bone loss in patients with ankylosing spondylitis. Rheumatology, 2020, 59, 1159-1169.	1.9	16
13	Ginsenoside Re Treatment Attenuates Myocardial Hypoxia/Reoxygenation Injury by Inhibiting HIF-1α Ubiquitination. Frontiers in Pharmacology, 2020, 11, 532041.	3.5	12
14	Cover Image, Volume 53, Issue 3. Cell Proliferation, 2020, 53, e12807.	5.3	0
15	Alteration of calcium signalling in cardiomyocyte induced by simulated microgravity and hypergravity. Cell Proliferation, 2020, 53, e12783.	5.3	24
16	Effects of spaceflight on the composition and function of the human gut microbiota. Gut Microbes, 2020, 11, 807-819.	9.8	32
17	Panax quinquefolium saponin attenuates cardiac remodeling induced by simulated microgravity. Phytomedicine, 2019, 56, 83-93.	5.3	12
18	Personalized Epigenome Remodeling Under Biochemical and Psychological Changes During Long-Term Isolation Environment. Frontiers in Physiology, 2019, 10, 932.	2.8	12

Shukuan Ling

#	Article	IF	CITATIONS
19	NDUFAB1 confers cardio-protection by enhancing mitochondrial bioenergetics through coordination of respiratory complex and supercomplex assembly. Cell Research, 2019, 29, 754-766.	12.0	66
20	Hematopoietic stem cells and lineage cells undergo dynamic alterations under microgravity and recovery conditions. FASEB Journal, 2019, 33, 6904-6918.	0.5	20
21	TMCO1-mediated Ca2+ leak underlies osteoblast functions via CaMKII signaling. Nature Communications, 2019, 10, 1589.	12.8	38
22	AAV-Anti-miR-214 Prevents Collapse of the Femoral Head in Osteonecrosis by Regulating Osteoblast and Osteoclast Activities. Molecular Therapy - Nucleic Acids, 2019, 18, 841-850.	5.1	24
23	The mechanosensitive Piezo1 channel is required for bone formation. ELife, 2019, 8, .	6.0	228
24	Myocardial CKIP-1 Overexpression Protects from Simulated Microgravity-Induced Cardiac Remodeling. Frontiers in Physiology, 2018, 9, 40.	2.8	17
25	The effect of Bu Zhong Yi Qi decoction on simulated weightlessness-induced muscle atrophy and its mechanisms. Molecular Medicine Reports, 2017, 16, 5165-5174.	2.4	14
26	The regulation of iron metabolism by hepcidin contributes to unloading-induced bone loss. Bone, 2017, 94, 152-161.	2.9	57
27	Dammarane Sapogenins Ameliorates Neurocognitive Functional Impairment Induced by Simulated Long-Duration Spaceflight. Frontiers in Pharmacology, 2017, 8, 315.	3.5	42
28	Circulating microRNAs Correlated with Bone Loss Induced by 45 Days of Bed Rest. Frontiers in Physiology, 2017, 8, 69.	2.8	14
29	Current Understanding of the Pathophysiology of Myocardial Fibrosis and Its Quantitative Assessment in Heart Failure. Frontiers in Physiology, 2017, 8, 238.	2.8	145
30	Simulated Microgravity and Recovery-Induced Remodeling of the Left and Right Ventricle. Frontiers in Physiology, 2016, 7, 274.	2.8	23
31	Late Gadolinium Enhancement Amount As an Independent Risk Factor for the Incidence of Adverse Cardiovascular Events in Patients with Stage C or D Heart Failure. Frontiers in Physiology, 2016, 7, 484.	2.8	15
32	Osteoclast-derived microRNA-containing exosomes selectively inhibit osteoblast activity. Cell Discovery, 2016, 2, 16015.	6.7	239
33	Circulating microRNAs correlated with the level of coronary artery calcification in symptomatic patients. Scientific Reports, 2015, 5, 16099.	3.3	59
34	CD44 deficiency inhibits unloading-induced cortical bone loss through downregulation of osteoclast activity. Scientific Reports, 2015, 5, 16124.	3.3	23
35	miR-214 promotes osteoclastogenesis by targeting Pten/PI3k/Akt pathway. RNA Biology, 2015, 12, 343-353.	3.1	198
36	Chronic Treatment With Ticagrelor Limits Myocardial Infarct Size. Arteriosclerosis, Thrombosis, and Vascular Biology, 2014, 34, 2078-2085.	2.4	115

Shukuan Ling

#	Article	IF	CITATIONS
37	PTEN Upregulation May Explain the Development of Insulin Resistance and Type 2 Diabetes with High Dose Statins. Cardiovascular Drugs and Therapy, 2014, 28, 447-457.	2.6	25
38	HDAC4 protects cells from ER stress induced apoptosis through interaction with ATF4. Cellular Signalling, 2014, 26, 556-563.	3.6	37
39	Dickkopf-1 (DKK1) phosphatase and tensin homolog on chromosome 10 (PTEN) crosstalk via microRNA interference in the diabetic heart. Basic Research in Cardiology, 2013, 108, 352.	5.9	31
40	Modulation of microRNAs in hypertension-induced arterial remodeling through the β1 and β3-adrenoreceptor pathways. Journal of Molecular and Cellular Cardiology, 2013, 65, 127-136.	1.9	39
41	MicroRNA-dependent cross-talk between VEGF and HIF1α in the diabetic retina. Cellular Signalling, 2013, 25, 2840-2847.	3.6	59
42	miR-214 targets ATF4 to inhibit bone formation. Nature Medicine, 2013, 19, 93-100.	30.7	495
43	Phosphodiesterase-3 inhibition augments the myocardial infarct size-limiting effects of exenatide in mice with type 2 diabetes. American Journal of Physiology - Heart and Circulatory Physiology, 2013, 304, H131-H141.	3.2	21
44	Nebivolol Induces Distinct Changes in Profibrosis MicroRNA Expression Compared With Atenolol, in Salt-Sensitive Hypertensive Rats. Hypertension, 2013, 61, 1008-1013.	2.7	37
45	Application of Molecular Imaging in Transgenic Animals. Advanced Topics in Science and Technology in China, 2013, , 661-670.	0.1	0
46	Regulation of phosphatase and tensin homolog on chromosome 10 in response to hypoxia. American Journal of Physiology - Heart and Circulatory Physiology, 2012, 302, H1806-H1817.	3.2	20
47	CKIP-1 Inhibits Cardiac Hypertrophy by Regulating Class II Histone Deacetylase Phosphorylation Through Recruiting PP2A. Circulation, 2012, 126, 3028-3040.	1.6	72
48	Phosphodiesterase III Inhibition Increases cAMP Levels and Augments the Infarct Size Limiting Effect of a DPP-4 Inhibitor in Mice with Type-2 Diabetes Mellitus. Cardiovascular Drugs and Therapy, 2012, 26, 445-456.	2.6	25
49	Redox Regulation of Actin by Thioredoxin-1 Is Mediated by the Interaction of the Proteins <i>via</i> Cysteine 62. Antioxidants and Redox Signaling, 2010, 13, 565-573.	5.4	32
50	Reduced function and disassembled microtubules of cultured cardiomyocytes in spaceflight. Science Bulletin, 2008, 53, 1185-1192.	9.0	12
51	Reduced function and disorganized cytoskeleton of cardiomyocytes in spaceflight. , 2006, , .		0